R-3

VMn underlayer for CoCrPt Longitudinal Media

S. C. Oh and T. D. Lee
Department of Materials Science and Engineering, Korea Advanced Institute of Science and Technology

Abstract

In this study, effects of novel VMn underlayer on magnetic properties of CoCrPt/VMn longitudinal medium was studied and compared with those of CoCrPt/Cr medium. It was found that the VMn film had (200) preferred orientation and the lattice constant was about 0.2967 nm, which is slightly larger than that of the Cr, 0.2888 nm. The grain size of VMn film was 9.3 nm at 30 nm thickness, and this is about 38 % smaller than that of a similarly deposited Cr film. The CoCrPt/VMn films showed higher coercivity in comparison with the CoCrPt/Cr films. The coercivity increase seems to be attributed to the increased Co (11.0) texture, improved lattice matching between Co (11.0) and VMn(200), and lower stacking fault density. Mn must have diffused into the CoCrPt magnetic layer more uniformly rather than preferentially along grain boundaries this reduced Ms at higher substrate temperature

I. INTRODUCTION

The demand for rapidly increasing recording densities in longitudinal thin film media requires both higher coercivity and lower noise. For high recording density and low noise, it is necessary to control the microstructure of Co-alloy film, such as grain size, crystallographic texture and grain isolation. The microstructure of Co-alloy film is greatly influenced by its underlayer. Accordingly, many researches have been focused on studied of the underlayers recently. In order to decrease grain size and to promote grain-to-grain epitaxial growth of Co-alloy by adjusting lattice constant of BCC Cr underlayer, Cr alloys with substitutional elements such as V[1], Mo[2], and Ti[3] have been investigated. Lately, CrMn underlayer has been explored to improve grain isolation [4].

In this study, a new type underlayer for CoCrPt longitudinal recording media will be reported. The VMn underlayer was investigated as a substitute for Cr or Cr alloys.

Equilibrium phase diagram shows Vanadium can dissolve about 53 at% Mn at 600 °C and retain a stable BCC structure. Also the lattice parameter of the VMn underlayer can be controlled by Mn contents.

II. EXPERIMENTAL

The effects of deposition temperature and underlayer thickness on the texture and magnetic properties were studied. Cr and VMn films were deposited onto glass substrates or thermally oxidized Si substrates and subsequently CoCrPt films were deposited by a DC magnetron sputtering method. Cr underlayers were studied for comparison purpose. The Ar sputtering pressure was 10 mTorr and the base pressure was about 1×10^{-6} Torr. The CoCrPt composition was controlled by a $CoCr_{19}$ alloy target with bonded Pt chips while the VMn films were deposited with pure Mn target with bonded V chips.

The compositions of the films were determined by energy dispersive x-ray spectrometry (EDX). The film texture was studied by standard x-ray diffractometry of θ-2θ scan with Cu Kα radiation. The stacking fault probabilities of films were analyzed by grazing incidence x-ray scattering using a synchrotron radiation source. Magnetic properties of the thin films were measured by a VSM at room temperature. ΔM measurements were performed with an alternating gradient magnetometer (AGM). Transmission electron microscopy (TEM) was used to characterize the grain size and its size distribution.

III. RESULTS AND DISCUSSION

Fig 1. shows the in-plane bright field TEM images of 30 nm thickness Cr and VMn underlayers deposited onto the Si substrates. The Cr showed an average grain size of 15 nm with the standard deviation of 4.36 nm while VMn showed an average grain size of 9.3 nm with the standard deviation of 2.34 nm. This uniform and fine grain of VMn underlayer may be more beneficial because it renders the probability of finer Co grain. Whether the CoCrPt film can inherit the uniform and fine grain will be investigated in our future work.

EDX analyses showed nm) that the VMn film had a composition of 71.3 at% V and 28.7 at% Mn and the CoCrPt film had a composition of 70.6 at% Co, 17.2 at% Cr and

12.2 at% Pt.

The in-plane Hc and S* values of CoCrPt (20 nm)/Cr (30 nm) and CoCrPt (20 nm)/VMn (30 nm) films with varying the substrate temperature are shown in Fig.2. The Hc values were at least 800 Oe higher for the all heated films with the VMn underlayers than the corresponding films with the Cr underlayers. A maximum Hc of 2500 Oe was obtained in the films with the VMn underlayer in comparison to 1500 Oe in that with the Cr underlayer. The S* values of CoCrPt/VMn films were also higher.

To understand the origin of the Hc and S* value increase, structural analyses of the CoCrPt/Cr and CoCrPt/VMn films were done.

Standard x-ray θ-2θ scan of the above films is shown in Fig. 3. The substrate heating up to 275 °C induced (200) texture in the VMn and Cr underlayers. As anticipated, these (200) Cr and (200) VMn textures induced the epitaxial growth of (11.0) CoCrPt texture. The (200) VMn intensity was smaller than that of Cr while the (11.0) intensity of CoCrPt deposited onto VMn film was stronger. This indicates that the CoCrPt/VMn films have better in-plane c-axis orientation than the CoCrPt/Cr films.Fig. 4 shows the grazing incidence XRD patterns of the CoCrPt/Cr and CoCrPt/VMn films deposited at the substrate temperature of 275 °C. These XRD patterns show the strong prominence of the Co (00.2) peak, consistent with the dominant (11.0) texture of the CoCrPt. From (10.0), (10.2), and (10.3) peak widths, the deformation and growth fault probabilities (α and β, respectively) were calculated as reported other paper [5]. In addition to these data, the areal misfit between the (11.0) magnetic plane and the (200) plane of underlayers are given in Table 1.

Table 1. Lattice constant, areal misfit, and stacking fault density ((α and β) in CoCrPt/Cr and CoCrPt/VMn films.

Sample	CoCrPt/Cr (a_{Cr} = 2.888 Å)	CoCrPt/VMn (a_{VMn} = 2.967 Å)
a	2.5809 Å	2.5804 Å
c	4.1897 Å	4.1833 Å
α	0.08	0.04
β	0.04	0.05
areal misfit	12.27 %	6.19 %

It has been reported that the origins of stacking faults can be associated with high platinum content, poor epitaxy to the underlayers, or the contamination of the sputtering gas by nitrogen or other impurities [5]. Accordingly, the lower fault density of CoCrPt/VMn films due to the improved lattice matching results in the better crystalline perfection. This may to be in part attributable to the Hc increase, in addition to the increased (11.0) texture.

The Ms and ΔM values were measured. The Ms values for CoCrPt/Cr and CoCrPt/VMn films are plotted against the substrate temperature in Fig. 5 (a). For CoCrPt/VMn films, the Ms values slightly decreased with the increasing substrate temperature up to 200 °C but further increase of the substrate temperature from 200 °C to 350 °C resulted in the sharp decrease of Ms values. However, for the CoCrPt/Cr films, no significant change in Ms was observed. This is probably due to the diffusion of Mn into the CoCrPt magnetic layer.

ΔM curves of 20 nm thick CoCrPt films on 30 nm Cr and VMn underlayers are shown in Fig. 5(b). A positive peak in a ΔM curve indicates the existence of exchange coupling between the grains in magnetic layer and its height is related to the degree of coupling. Judging from Fig. 5(b), the film with a VMn underlayer had about the same exchange coupling as the film with a Cr underlayer. The above two results suggest that Mn may be diffused into the CoCrPt magnetic layer more uniformly rather than preferentially along grain boundaries.

Fig. 6 shows changes of Hc and S* values of 20 nm thick CoCrPt films with varying the underalyer thickness at the substrate of 275 °C. In the both cases, the Hc values increased and then reached a plateau with increasing the underlayer thickness.

The Hc and S* values of CoCrPt (20 nm)/Cr (30nm) and CoCrPt (20 nm)/VMn(30 nm) films with increasing dc substrate bias voltage are shown in Fig. 7(a). The bias voltage was applied during deposition of magnetic layer and underlayer. The Hc values increased with the bias voltage, in the both CoCrPt/Cr and CoCrPt/VMn films. The maximum Hc value was obtained in the CoCrPt/VMn films deposited at the substrate bias voltage of –400 V. The application of substrate bias has shifted the Co (11.0) peak position by 0.4°. Fig. 7(b) shows Co (11.0) peak shift with substrate bias voltage in the CoCrPt/VMn films. This peak shift is attributed to expansion in lattice constant of the CoCrPt magnetic layer due to change of composition associated with difference in sputtering yields among the components.

One of the reasons for the coercivity increase in the bias sputtered specimens is higher Pt contents. The other reasons may be such factors as changes in texture formation, grain size, segregation mode and defects. The change in texture formation with increasing applied bias voltage is under investigation.

IV. CONLUSIONS

The VMn underlayer showed finer and more uniform grain size distribution than the Cr underlayer. The use of VMn underlayers can obtain higher Hc than pure Cr underlayer. The origin of Hc increase may be associated with the increased Co (11.0) texture, improved lattice matching between Co (11.0) and VMn (200) and lower stacking fault density. Judging from the measurement of Ms and ΔM, Mn seems to be diffused into the CoCrPt magnetic layer more uniformly rather than preferentially along grain boundaries. Coercivity in the both CoCrPt/VMn and CoCrPt/Cr films increased with increasing bias voltage. The coercivity may be due to changes in texture formation, grain size, segregation mode and defects, in addition to the higher Pt contents.

ACKNOWLEDGMENTS

The authors would like to thank Dr. H. J. Lee and Mr. H. Ryu of Korea Research Institute of Standards and Science for TEM observation and prof. K. B. Lee of Phong University of Science and Technology for measurements of GIXRD.

REFERENCES

[1] M. A. Parker, J. K. Howard, R. Ahlert and K. R. Coffey, J. Appl. Phys., 73, pp. 5660-5662 (1993)

[2] E.N. Abarra, T. Suzuki. IEEE. Trans. Magn., 33, pp. 2995-2997 (1997)

[3] Y. Shiroishi, Y. Hosoe, A. Ishikawa, Y. Yashisa, Y. Sugita, H. Suzuki and Y. Ohno and M. Ohura, J. Appl. Phys., 73, pp. 5569-5571 (1993)

[4] L. L. Lee, D. E. Laughlin and D. N. Lambeth, IEEE. Trans. Magn., 34, pp. 1561-1563 (1998)

[5] P. Dova, H. Laidler, K. O'Grady, M. F. Toney and M. F. Doerner, J. Appl. Phys., 85, pp. 2775-2781 (1999)

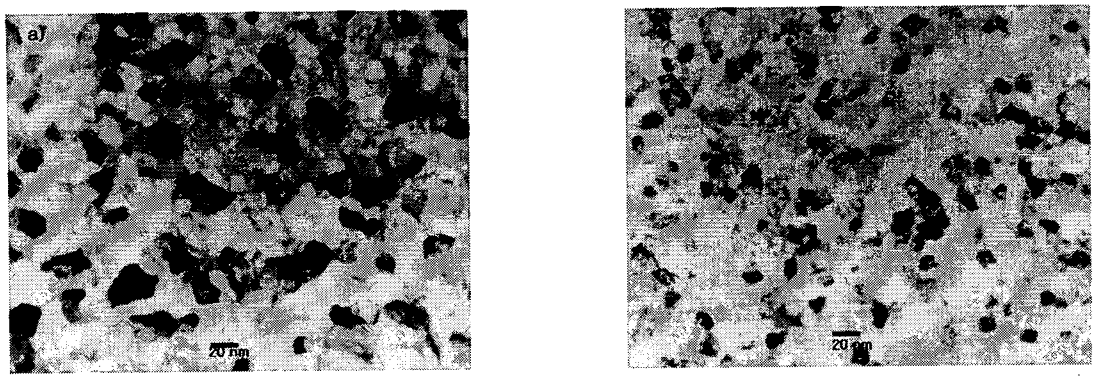

Fig. 1 TEM bright field images of (a) Cr (30 nm) and (b) VMn (30 nm)

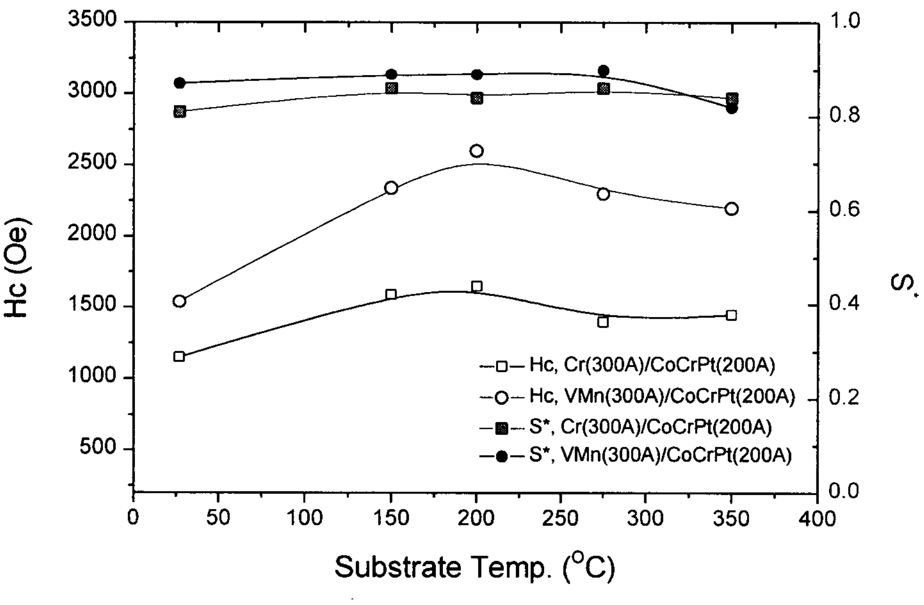

Fig. 2 In-plane Hc and S* of CoCrPt(20 nm)/Cr(30 nm) and CoCrPt(20nm)/VMn (30nm) films with substrate temperature

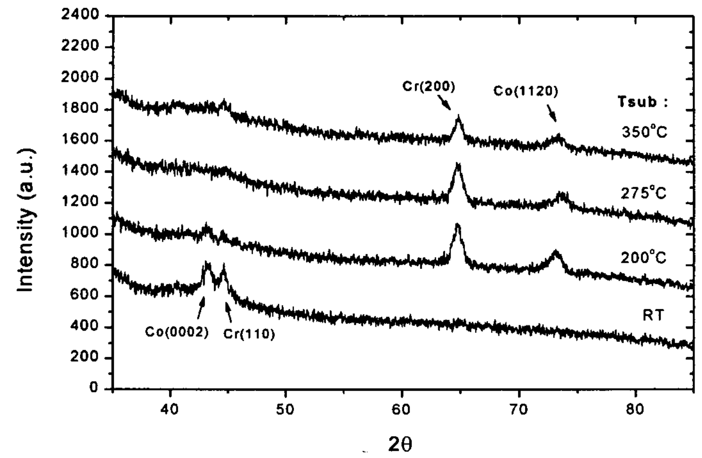

(a)

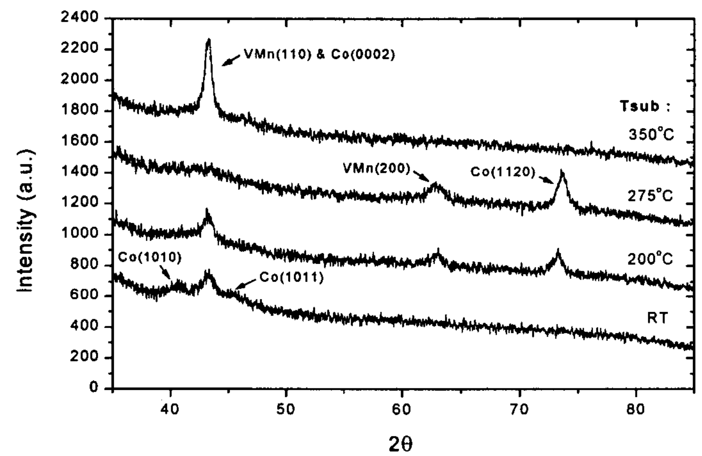

(b)

Fig. 3 X-ray patterns of (a) CoCrPt(20 nm)/Cr(30 nm) and (b) CoCrPt(20 nm)/VMn(30 nm) with substrate temperature

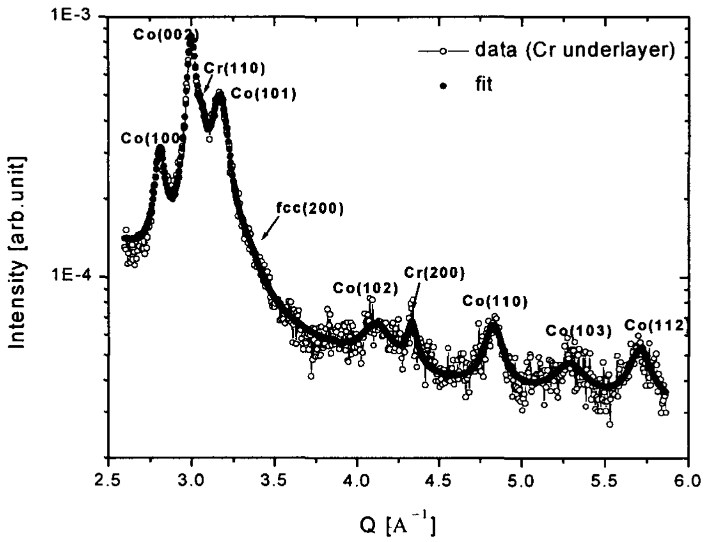

(a)

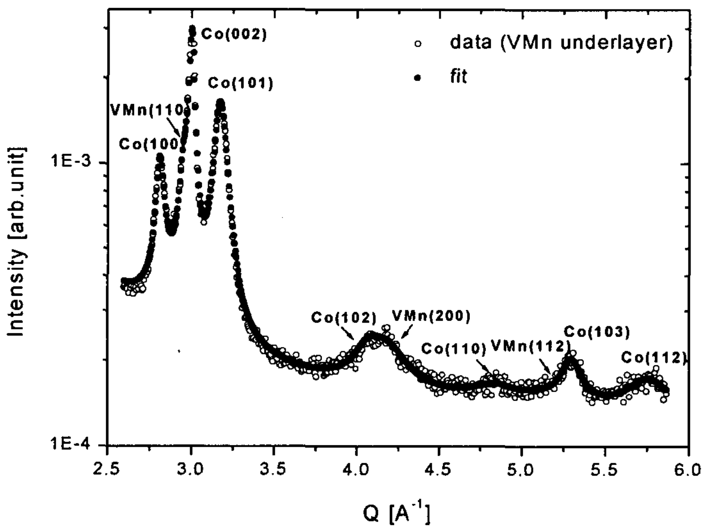

(b)

Fig. 4 Grazing incidence x-ray patterns of (a) CoCrPt(20 nm)/Cr(30 nm) and (b) CoCrPt(20nm)/VMn(30 nm)deposited at substrate temperature of 275°C; incident beam energy = 7.6KeV, incident angle=0.55

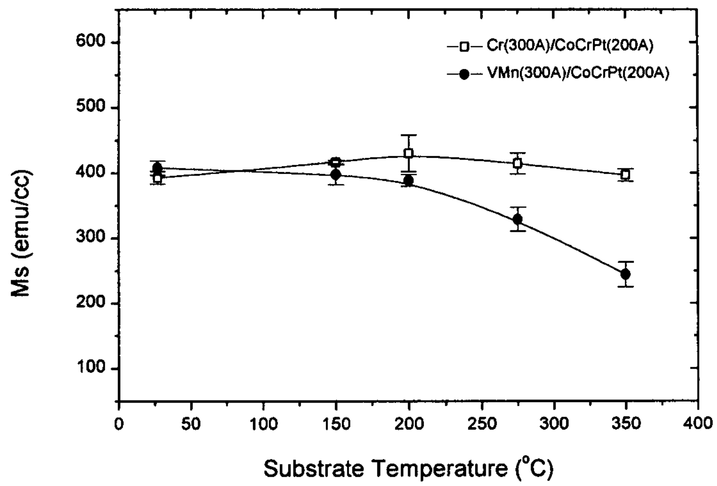

(a)

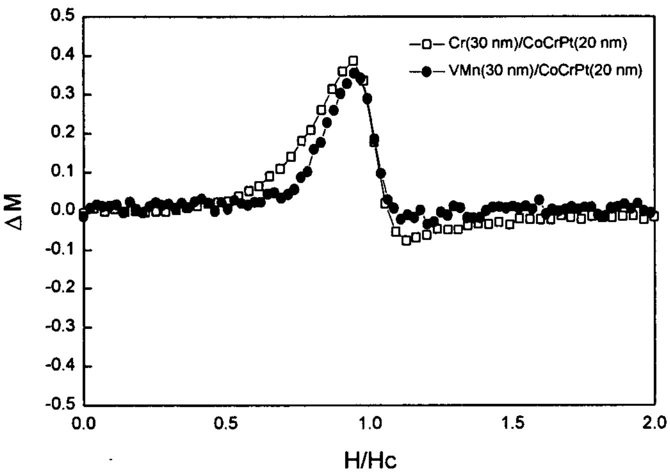

(b)

Fig. 5 (a) Ms values of CoCrPt/Cr and CoCrPt/VMn films with substrate temperature, (b) ΔM curvesof the CoCrPt films deposited on Cr and VMn underlayer at substrate temperature of 275 °C·

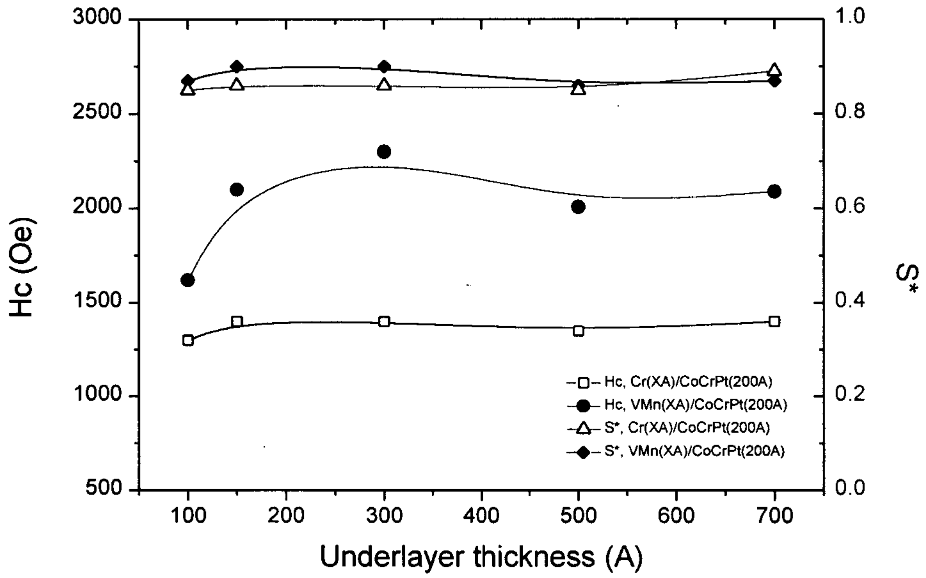

Fig. 6 Hc and S* values of 20 nm thick CoCrPt films deposited on various thicknesses of VMn or Cr underlayers at substrate temperature of 275 °C

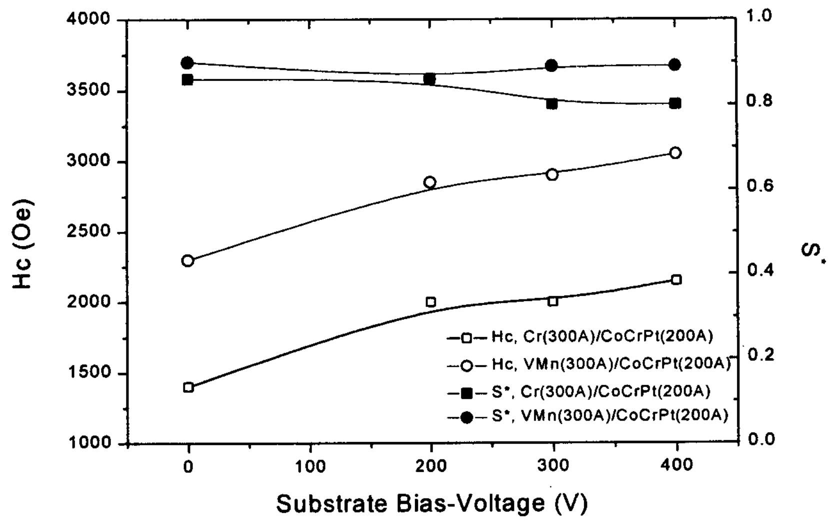

(a)

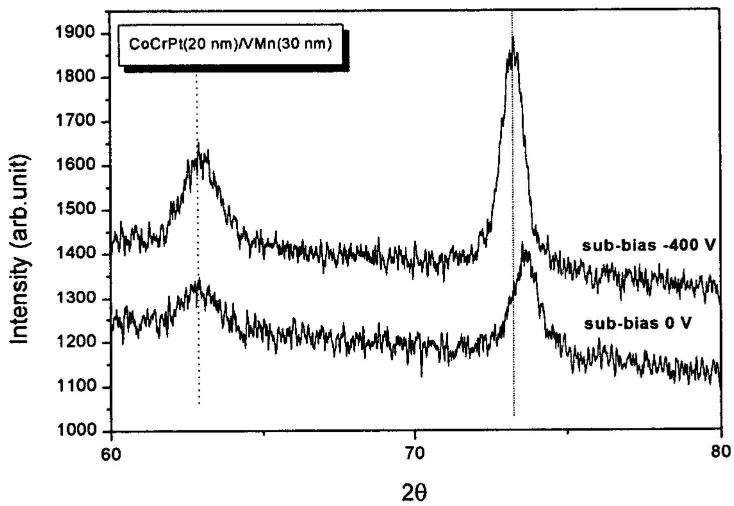

(b)

Fig. 7 (a) Hc and S* values of CoCrPt (20 nm)/Cr (30nm) and CoCrPt (20 nm)/VMn(30 nm) films with substrate bias voltage, (b) (1120) peak position shift with substrate bias voltage